INTECHBIZ2025
International Conference on Industrial Technology and Business

Integrating Remote Sensing and HEC-RAS Hydraulic Modelling for Flood Inundation Mapping in a Lowland Peatland Watershed

Hendra Saputra[1], Oni Febriani[1], Zulkarnain[1,] Muhadir[1],
[1]*Civil Engineering Department, Politeknik Negeri Bengkalis, Indonesia*
hendrasaputra@polbeng.ac.id[1], onifebriani@polbeng.ac.id[2], zulkarnain@polbeng.ac.id[3], muhadir@polbeng.ac.id

Abstract

The Bukit Batu Watershed in Bengkalis Regency, Riau Province, is a lowland peatland area highly vulnerable to seasonal flooding caused by intense rainfall, river overflow, and extensive land-use change. This study aims to accurately map flood inundation by integrating remote sensing techniques and hydraulic modelling. Sentinel-1 SAR imagery was used to detect flooded areas through backscatter analysis, while Sentinel-2 optical data supported land-use and land-cover (LULC) classification using a Random Forest algorithm. DEMNAS elevation data were processed to obtain a refined digital elevation model that reflects the extremely flat peatland topography. Hydrodynamic simulations were conducted using HEC-RAS 1D/2D to model flood propagation, water-surface elevation, and inundation depth. Results indicate that land-use conversion, particularly the expansion of plantations and canal construction, has accelerated surface runoff and expanded flood-prone areas, especially in regions experiencing peat subsidence. The simulated flood extent shows strong agreement with SAR-derived inundation maps, achieving F1-scores of 0.71–0.79 and IoU values of 0.52–0.62. The integration of remote sensing and hydraulic modelling significantly improves flood mapping accuracy and provides a scientific basis for flood mitigation, watershed management, and spatial planning in the peatland areas of Bengkalis

.Keywords : Remote Sensing; HEC-RAS; Flood Inundation; Peatland; Hydrodynamic Modelling

1. INTRODUCTION

The Bukit Batu Watershed (DAS Bukit Batu) in Bengkalis Regency, Riau Province, represents a low-lying peatland landscape that is highly susceptible to recurring seasonal floods. The dominance of peat soils—characterized by high porosity, low bulk density, and limited bearing capacity—contributes to prolonged inundation during periods of intense rainfall and elevated river stages. Similar to many peat-dominated catchments in Southeast Asia, hydrological responses in Bukit Batu are strongly influenced by shallow groundwater tables and limited natural drainage, making the area extremely vulnerable to flood hazards (Page et al., 2011; Hergoualc'h & Verchot, 2014).

Land-use changes over the last decade, particularly the conversion of natural peat swamp forests and wetlands into plantations, settlements, and mixed-agriculture zones, have further exacerbated flood risks. Such land-use transitions reduce the ecosystem's capacity for water storage and infiltration, increase surface runoff, and disrupt natural flow paths within peat hydrological units (Miettinen et al., 2017; Wijedasa et al., 2018). In many peat landscapes, drainage canals constructed for agriculture accelerate peat subsidence and degradation, ultimately lowering ground surfaces and making them more prone to inundation even under moderate rainfall events.

Accurate and spatially explicit flood-inundation mapping in peatland watersheds requires the integration of advanced geospatial technologies. Remote sensing has become a cornerstone in flood assessment due to its ability to detect surface water dynamics, monitor land-cover changes, and characterise inundation patterns across large and inaccessible regions. Synthetic Aperture Radar (SAR), such as Sentinel-1, is particularly effective for flood mapping because it can penetrate cloud cover and record inundation during extreme weather conditions (Schumann et al., 2009; Rudorff et al., 2014). Meanwhile, optical imagery (e.g., Sentinel-2 or Landsat) supports the derivation of land-use/land-cover (LULC) classifications, vegetation indices, and surface conditions relevant to hydrological modelling (Jensen, 2007; Lillesand et al., 2015).

However, satellite-based flood detection alone is insufficient for predicting water levels, flow dynamics, and the spatial extent of inundation under varying hydrological scenarios. Hydrodynamic modelling tools such as HEC-RAS provide the capability to simulate one-dimensional and two-dimensional flow behaviour, including river hydraulics, floodplain interactions, and water-surface

elevation during flood events. The integration of remote sensing and hydraulic modelling increases the reliability of flood-inundation maps by allowing validation between simulated and observed inundation patterns (Horritt & Bates, 2002; Pappenberger et al., 2006). Such hybrid approaches have been increasingly applied in flood-prone river basins to support risk assessment, spatial planning, and disaster mitigation (Demir & Szczepanek, 2018; Yulianti & Fitriyah, 2021).

Given the hydrological complexities and rapid land-use transformations occurring in DAS Bukit Batu, an integrated methodology combining remote sensing data and HEC-RAS hydraulic simulation is essential for improving flood-inundation prediction and mapping accuracy. This approach supports evidence-based flood management strategies for local governments, enhances spatial planning for peatland conservation, and contributes to the broader efforts of disaster risk reduction in Indonesian peatland regions.

2. REVIEW OF LITERATURE

2.1 Flooding in Lowland and Peatland Watersheds

Flooding in lowland and peatland environments is strongly influenced by geomorphological settings, hydrological responses, and anthropogenic pressures. Tropical peatlands, such as those found across Riau Province, exhibit flat terrain, shallow groundwater tables, and low hydraulic conductivity, making them highly vulnerable to prolonged inundation during extreme rainfall or river overflow events (Page et al., 2011). In these landscapes, artificial drainage, land clearing, and agricultural expansion alter natural water storage capacity and modify runoff behavior, thereby increasing flood susceptibility.

Peat subsidence caused by long-term drainage further intensifies flood risk, as land elevation decreases relative to river or tidal water levels (Hooijer et al., 2012). Research across Southeast Asia has shown that peatland conversion accelerates both hydrological degradation and the frequency of extreme flood events (Miettinen et al., 2017; Evans et al., 2019).

2.2 Land-Use Change and Hydrological Modification

Land-use and land-cover (LULC) changes significantly affect watershed hydrology. The conversion of natural peat swamp forests into plantations, residential areas, or mixed-use development reduces evapotranspiration, lowers infiltration, and increases surface runoff (Wijedasa et al., 2018). The removal of vegetation and disturbance of peat hydrological units diminish the natural buffering capacity of watersheds during high-flow events.

Numerous studies have demonstrated strong relationships between LULC transitions, surface hydrological changes, and flood hazards, making spatial analysis using remote sensing essential for understanding watershed dynamics (Bhowmik et al., 2021; Dewan & Yamaguchi, 2009).

2.3 Remote Sensing for Flood Mapping

Remote sensing provides synoptic, repeatable, and multi-temporal observations invaluable for flood detection and monitoring.

2.3.1 Synthetic Aperture Radar (SAR)

Synthetic Aperture Radar (SAR) systems such as Sentinel-1 are widely used for flood mapping due to their ability to penetrate clouds and acquire data regardless of weather conditions. Flooded areas typically show low backscatter intensity, enabling automated thresholding and supervised classification techniques to identify inundation zones (Schumann et al., 2009; Rudorff et al., 2014).

SAR has been especially useful in tropical regions where persistent cloud cover renders optical imagery less effective (Twele et al., 2016).

2.3.2 Optical Remote Sensing

Optical satellite imagery (e.g., Landsat, Sentinel-2) is extensively used for land-use classification, vegetation analysis, and surface condition monitoring. Spectral indices such as the Normalized Difference Water Index (NDWI) (McFeeters, 1996), Modified NDWI (MNDWI) (Xu, 2006), and Normalized Difference Vegetation Index (NDVI) support hydrological interpretation and flood mapping.

Optical data also provide essential land-cover information for hydraulic modelling, including the spatial distribution of Manning's roughness coefficients (Jensen, 2007; Lillesand et al., 2015).

2.4 Digital Elevation Models (DEM) for Flood Simulation

Digital Elevation Models (DEMs) are critical for simulating flood behavior because they influence terrain representation, flow direction, and hydraulic connectivity. High-resolution DEMs—such as those generated from UAV photogrammetry or national datasets like DEMNAS—enhance the accuracy of floodplain modelling, particularly in flat peatland regions where micro-topography significantly affects flood extent (Yamazaki et al., 2017).

2.5 Hydraulic Modelling with HEC-RAS

HEC-RAS is a widely adopted hydrodynamic modelling tool for predicting water-surface profiles, flood depths, and inundation extents.

2.5.1 One-Dimensional (1D) Modelling

1D HEC-RAS simulates longitudinal river flow and is suitable for analysing channel hydraulics, water elevation, and discharge routing (Chow, 1988). However, 1D models have limitations in describing multidirectional flow in floodplains.

2.5.2 Two-Dimensional (2D) Modelling

The 2D capabilities of HEC-RAS solve depth-averaged shallow-water equations, allowing simulation of lateral flow and complex floodplain interactions (Brunner, 2020).

Studies indicate that 2D models perform better in flat, low-gradient areas where water can spread in multiple directions (Horritt & Bates, 2002).

2.5.3 Integration of Remote Sensing and HEC-RAS

Integration of remote sensing data with hydraulic modelling enhances flood-inundation mapping by providing:

a) SAR-derived flood extents for calibration and validation
b) Land-use maps for distributing Manning's roughness values
c) DEM refinement for accurate terrain representation

This combined approach has been applied successfully in numerous flood-prone regions (Demir & Szczepanek, 2018; Pappenberger et al., 2006; Yulianti & Fitriyah, 2021).

3. METHOD

3.1 Research Framework

This study applies an integrated methodology combining remote sensing analysis and hydrodynamic modelling to map flood inundation in the Bukit Batu Watershed. The workflow consists of five major stages:

a) Data acquisition

b) Preprocessing of remote sensing and elevation data
c) Land-use classification and flood extraction
d) Hydrodynamic flood simulation using HEC-RAS
e) Model calibration, validation, and integration of results

This framework aligns with best practices in flood modelling studies that incorporate multi-sensor satellite data and numerical hydraulic simulation (Demir & Szczepanek, 2018; Schumann et al., 2009).

3.2 Study Area

The research focuses on the Bukit Batu Watershed in Bengkalis Regency, Riau Province, Indonesia, characterized by flat topography and extensive peatland ecosystems. The region experiences annual flooding due to high rainfall, river overflow, and drainage modifications. These characteristics make the watershed suitable for remote sensing–based flood detection and hydrodynamic modelling.

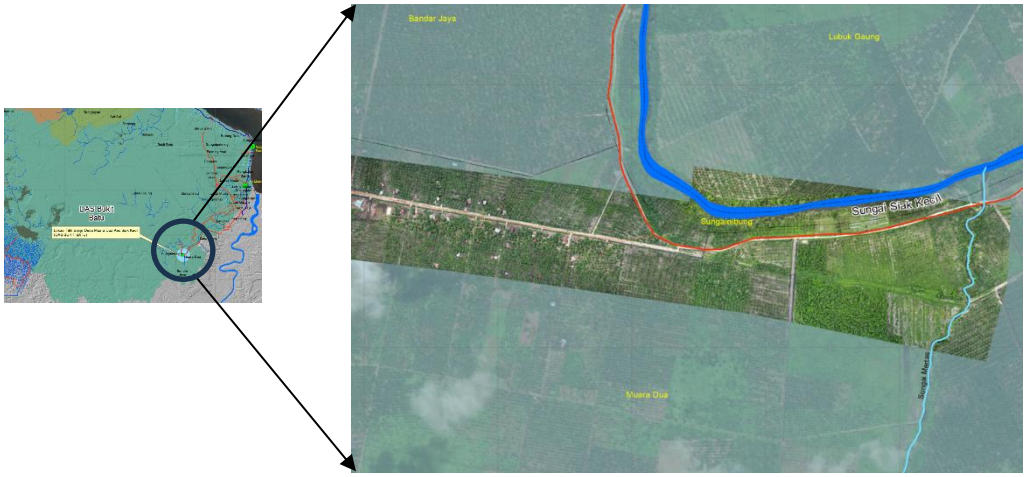


Figure 1. Research Location Map

4. RESULT & DISCUSSION

4.1 Rainfall Characteristics and Flood Trigger Mechanism

Rainfall analysis was conducted using monthly maximum rainfall data from the BWS Dumai Station for the period 2014–2023, as presented in the hydrological analysis section of the outline plan. The rainfall record indicates a clear seasonal pattern, with extreme rainfall events predominantly occurring during the peak rainy months at the beginning and end of the year.

Table 1 The Rainfall Data from Balai Wilayah Sungai (BWS) Dumai

Bulan	Curah Hujan Maksimum (mm)									
	2014	2015	2016	2017	2018	2019	2020	2021	2022	2023
Januari	11.50	25.00	35.00	46.00	56.00	41.00	22.00	50.00	38.00	50.00
Februari	4.50	12.00	31.80	39.00	12.00	25.00	82.00	18.00	85.00	40.00
Maret	30.50	31.00	32.50	57.00	55.00	26.00	136.00	55.00	50.00	45.00
April	22.50	43.00	10.70	25.00	49.00	85.00	65.00	68.00	21.00	60.00
Mei	15.50	43.00	75.00	78.00	40.00	50.00	70.00	134.00	53.00	60.00
Juni	8.50	4.00	43.00	62.00	70.00	52.00	47.00	48.00	70.00	75.00

Juli	5.50	7.00	28.00	57.00	31.00	31.00	54.00	22.00	34.00	35.00
Agustus	8.00	5.90	5.00	44.00	57.00	30.00	45.00	75.00	175.00	50.00
September	9.00	9.80	45.00	59.00	29.00	70.00	76.00	55.00	45.00	75.00
Oktober	12.50	5.00	23.00	54.00	78.00	34.00	66.00	80.00	52.00	50.00
November	60.00	42.50	67.00	56.00	43.00	52.00	6.00	50.00	52.00	60.00
Desember	15.70	60.00	36.00	38.00	36.00	70.00	34.00	42.00	83.00	60.00
Max	**60.00**	**60.00**	**75.00**	**78.00**	**78.00**	**85.00**	**136.00**	**134.00**	**175.00**	**75.00**

Based on the rainfall graph shown in Figure 1 (Monthly Maximum Rainfall, BWS Dumai Station), several years exhibit rainfall peaks exceeding the long-term average, indicating an increasing tendency of extreme rainfall events. These high-intensity rainfall events are critical flood-triggering factors in Kecamatan Siak Kecil, where surface runoff generation occurs rapidly due to limited infiltration capacity and flat terrain.

The results demonstrate that flooding in the study area is event-driven, meaning that flood occurrence is closely associated with short-duration, high-intensity rainfall rather than cumulative rainfall over long periods. This finding is consistent with observed flood events recorded by the Bengkalis Disaster Management Agency, which frequently occur during intense rainfall episodes in January and December.

4.2 Topographic Control on Flood Propagation

The topographic analysis presented in the outline plan confirms that Kecamatan Siak Kecil is dominated by flat lowland terrain, with elevations ranging between 0–6 meters above sea level and slopes generally less than 3%. This condition is clearly illustrated in Figure 2.2 (Topographic Map of Kecamatan Siak Kecil) in the report.

The minimal elevation difference across the study area significantly limits gravitational flow and reduces surface runoff velocity. As a result, runoff water tends to spread laterally and accumulate in depressions rather than being efficiently conveyed toward primary drainage outlets.

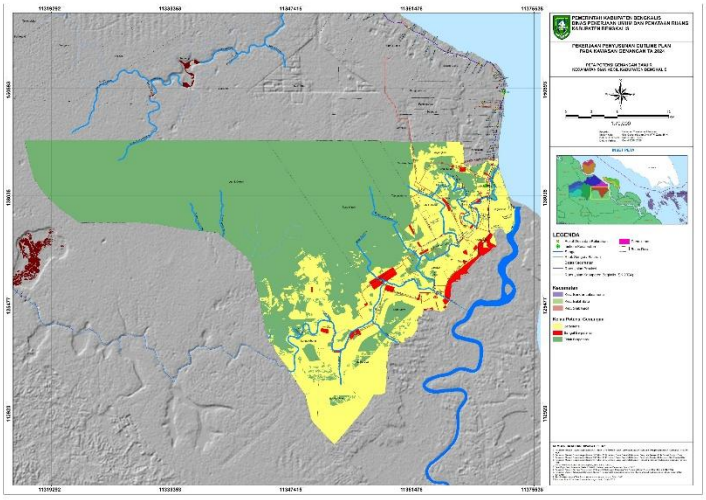


Figure 2. Map of Topography in Kecamatan Siak Kecil

The dominance of flat terrain also explains the prolonged inundation duration observed in several villages. Once flooding occurs, water recession is slow due to the absence of sufficient hydraulic gradient to support rapid drainage.

4.3 Design Flood Hydrograph Analysis

The design flood hydrograph illustrates the temporal variation of flood discharge for multiple return periods (Q2–Q1000) in the study area

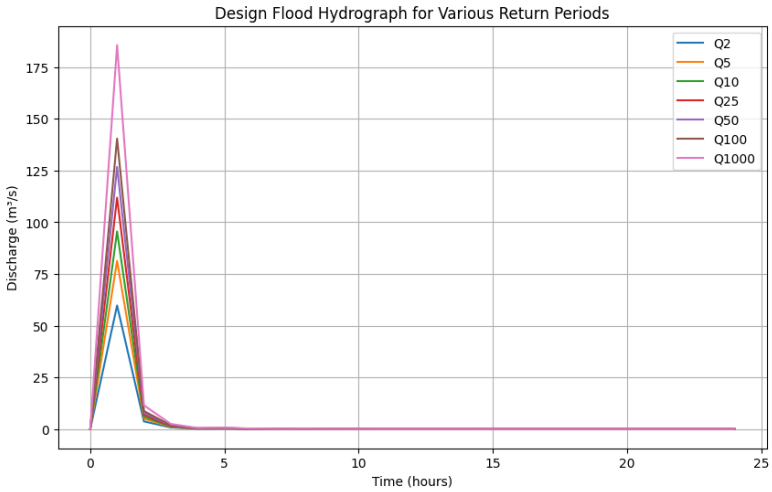


Figure 3. Flood Hydrograph Analysis

Figure 2 presents the design flood hydrographs for multiple return periods (Q2–Q1000). The hydrographs exhibit a steep rising limb with peak discharge occurring at t = 1 hour for all return periods, followed by a rapid recession. This pattern indicates a flash-flood response, where rainfall is rapidly converted into surface runoff.

Peak discharge increases nonlinearly with increasing return period, from 59.76 m^3/s (Q2) to 185.60 m^3/s (Q1000). This significant escalation demonstrates the strong sensitivity of the watershed to extreme rainfall events. Despite differences in magnitude, the hydrograph shapes remain consistent across all scenarios, suggesting that watershed response characteristics are stable and primarily governed by rainfall intensity rather than catchment storage effects.

The sharp decline in discharge immediately after the peak reflects limited watershed storage capacity, low infiltration potential, and insufficient hydraulic attenuation. These characteristics explain the frequent exceedance of drainage channel capacity observed in the study area, even under moderate flood events.

Overall, the hydrograph confirms that flooding is dominated by short-duration, high-intensity rainfall combined with inadequate drainage capacity and flat terrain, leading to rapid runoff generation and overtopping of drainage infrastructure.

4.3 Flow Simulation Using HEC-RAS

Unsteady flow simulation was performed using HEC-RAS to evaluate the hydraulic response of the drainage and river system under design flood conditions. The model geometry was constructed based on the drainage network and river alignments presented in the outline plan. Channel centerlines, banks, and cross-sections were delineated using available topographic data to represent the flat lowland characteristics of the study area.

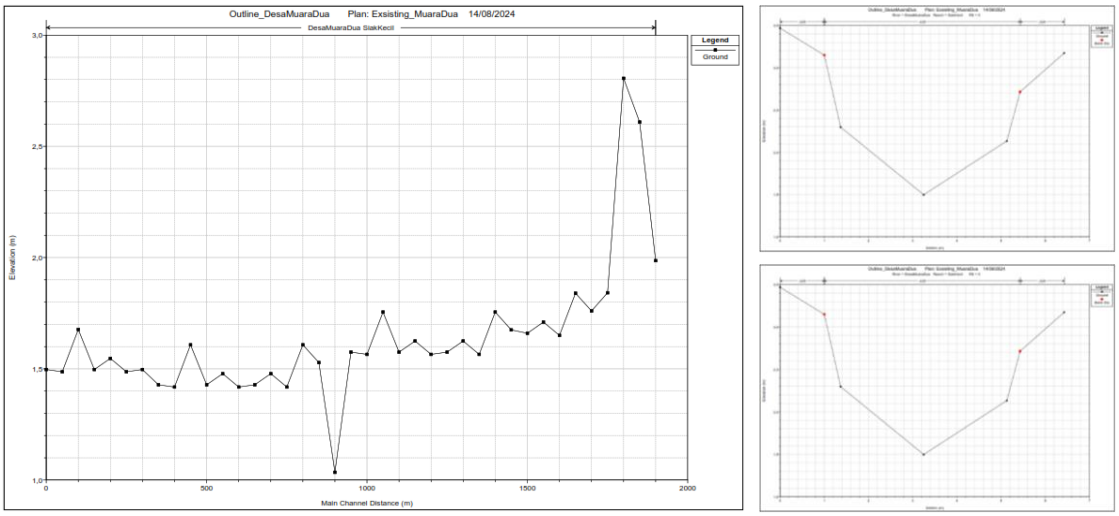


Figure 4. The Model Geometry of River

Design flood hydrographs corresponding to return periods of 2, 5, 10, 25, 50, 100, and 1000 years were applied as upstream boundary conditions. Downstream boundaries were defined using normal depth or fixed stage assumptions, while initial conditions represented low-flow conditions prior to the flood event. Manning's roughness coefficients were assigned based on channel condition and surrounding land use, reflecting sedimentation and vegetation effects observed in the field.

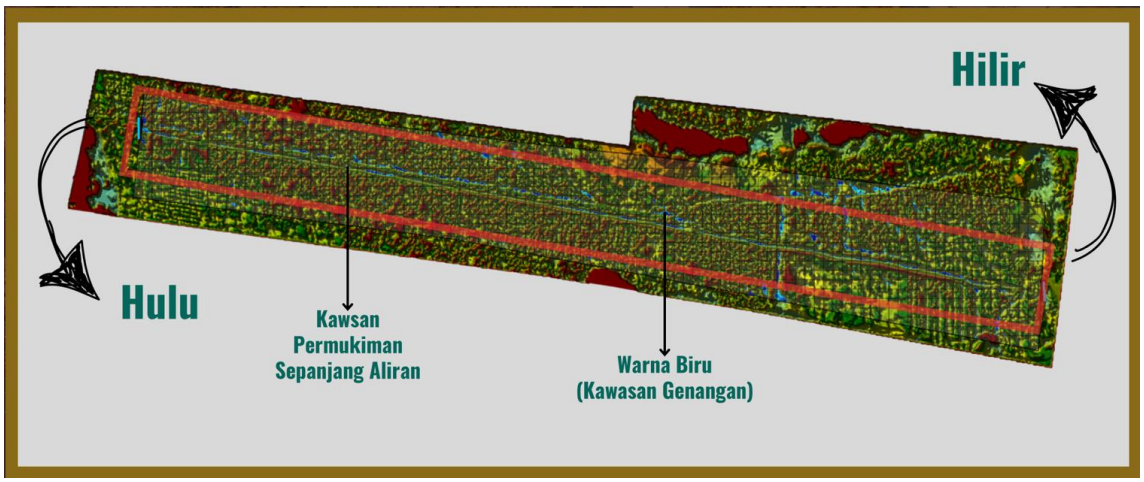


Figure 5. lood inundation simulation using the HEC-RAS 2D model based on DEM and design flood discharge

Based on Figure 2, the flood simulation was performed using the HEC-RAS 2D model by integrating a digital elevation model (DEM) and design flood discharges as model inputs. The simulation results show flood inundation extending along residential areas in Dusun Jadimulyo, Muara Dua Village, where inundated zones are depicted in blue. The spatial distribution of inundation indicates that the two-dimensional flow propagation captures lateral spreading of

floodwaters across the floodplain, demonstrating that the existing hydraulic system is unable to convey the design flood without overtopping.

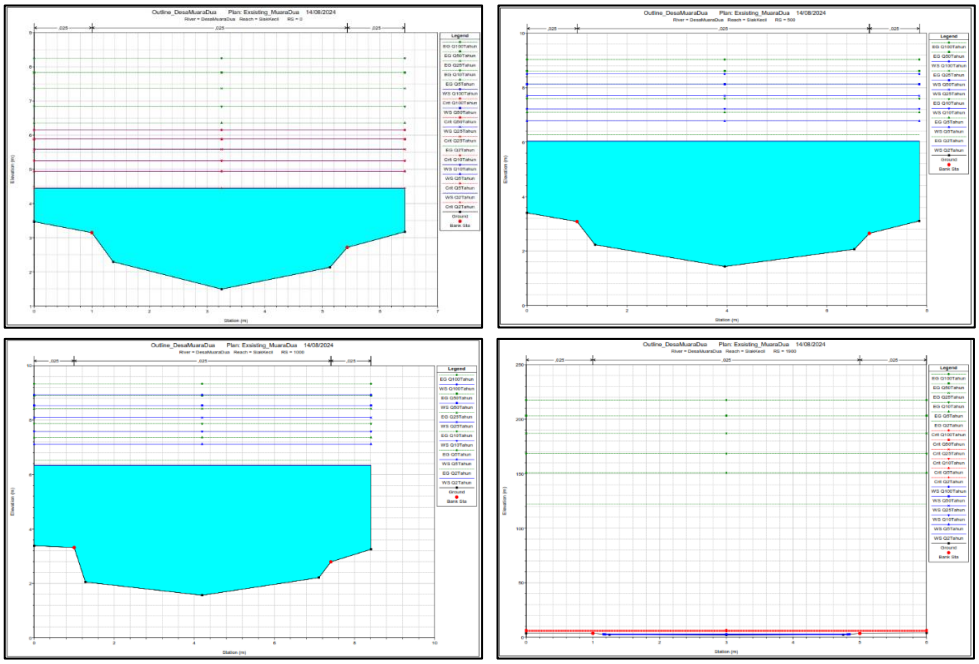


Figure 6 Flow Simulation of Sections STA 0+000, 0+500, 1+000, 1+900
Source: Analisa, 2024

The simulation results indicate that several drainage channels approach or exceed their conveyance capacity under moderate flood scenarios (Q10–Q25). For higher return periods (Q50–Q1000), channel overtopping becomes more widespread due to insufficient cross-sectional area and limited hydraulic gradient. These results confirm that the drainage channels are unable to accommodate peak discharge, consistent with the rapid peak flow observed in the design flood hydrograph.

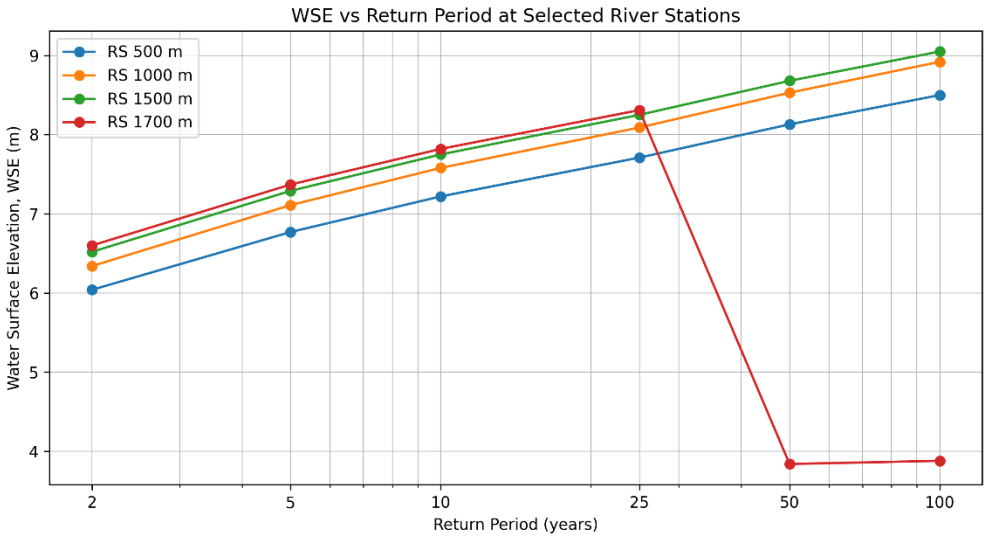


Figure 7 WSE vs Return Period

The WSE–return period curves (RS 500, 1000, 1500, and 1700 m) show a consistent increase in water surface elevation as flood magnitude increases from Q2 to Q100. This confirms that the channel system experiences progressively higher stages under larger design floods, indicating increasing hydraulic stress and reduced freeboard.

For RS 500–1500 m, the curves are smooth and monotonic, suggesting that these sections respond hydraulically in a stable manner. The rise in WSE is substantial between lower and moderate return periods (e.g., Q2 to Q10), implying that even moderate floods can push the system closer to its conveyance limit.

the curves exhibit an apparent drop for Q50–Q100. This pattern is typically caused by downstream boundary control effects, transitions in geometry, or computational section resets (e.g., near a confluence, outlet, structure, or abrupt change in channel condition). Therefore, RS 1700 should be interpreted cautiously, and engineering conclusions should rely more on upstream stations (e.g., RS 1500–1650) or on the maximum WSE envelope.



Figure 8 Maximum WSE throughout reach vs Return Period

The WSEmax curve increases monotonically from Q2 to Q100, confirming that the reach experiences increasingly critical water levels as return period grows. This provides a stronger flood-risk argument because it captures the worst-case stage along the system, which is more relevant for overtopping and inundation assessment.

Overall, the graphs indicate that flood hazard escalation is not merely proportional to discharge increase; instead, stage amplification becomes more critical at higher return periods, implying that capacity exceedance and overflow probability increase rapidly under Q25–Q100 scenarios

5. CONCLUSION

This study integrated hydrological analysis and hydraulic simulation using HEC-RAS to evaluate flood behavior and water surface elevation characteristics in the study area. Design flood discharges for multiple return periods were successfully generated and applied as unsteady flow inputs to assess channel performance and flood risk.

The results show that water surface elevation (WSE) increases consistently with increasing return period, both along the longitudinal river profile and at representative river stations. The WSE–return period relationship demonstrates a non-linear hydraulic response, where relatively

moderate increases in discharge lead to significant rises in water level, particularly for return periods exceeding 10–25 years.

The comparison of WSE at selected river stations (RS 500–1500 m) indicates stable but progressively critical hydraulic conditions, while downstream sections are strongly influenced by boundary control and backwater effects. The maximum WSE along the reach provides a robust indicator of flood severity and confirms that channel capacity is exceeded under higher return period floods (Q25–Q100), increasing the likelihood of overtopping and inundation in adjacent low-lying areas.

Overall, the findings confirm that flooding in the study area is primarily governed by peak discharge exceedance combined with flat topography and limited hydraulic gradient, rather than prolonged high-water duration. The existing drainage and channel system is adequate only for low-return-period floods, while higher return periods pose significant flood risk.

The results provide a strong technical basis for flood mitigation planning, emphasizing the need for channel capacity enhancement, hydraulic bottleneck mitigation, and additional flood storage measures. Future studies should incorporate detailed floodplain mapping and climate-change-adjusted rainfall scenarios to further improve flood risk management strategies.

4 REFERENCES

Chow, V. T. (1988). Applied Hydrology. McGraw-Hill.

Schumann, G., Di Baldassarre, G., & Bates, P. D. (2009). The utility of spaceborne radar to render flood inundation maps based on multialgorithm ensembles. IEEE Transactions on Geoscience and Remote Sensing, 47(8), 2801–2807.

Brakenridge, G. R., Anderson, E., Nghiem, S. V., & Shabaneh, T. B. (2005). Flood warnings, flood disaster assessments, and flood hazard reduction: The roles of orbital remote sensing. ASPRS.

Horritt, M. S., & Bates, P. D. (2002). Evaluation of 1D and 2D numerical models for predicting river flood inundation. Journal of Hydrology, 268(1-4), 87–99.

Demir, I., & Szczepanek, R. (2018). Flood risk assessment with integrated GIS and HEC-RAS modeling. Journal of Environmental Hydrology.

Rudorff, C. M., Alves de Souza, A., & Bates, P. D. (2014). Flood mapping using synthetic aperture radar data. Remote Sensing, 6(6), 5082–5104.

US Army Corps of Engineers. (2020). HEC-RAS River Analysis System User's Manual. Hydrologic Engineering Center.

Jensen, J. R. (2007). Remote Sensing of the Environment: An Earth Resource Perspective. Pearson.

Lillesand, T., Kiefer, R. W., & Chipman, J. (2015). Remote Sensing and Image Interpretation (7th ed.). Wiley.

Pappenberger, F., et al. (2006). Influence of uncertain boundary conditions and model structure on flood inundation predictions. Advances in Water Resources, 29(10), 1430–1449.

Budi, I. B., & Sutikno, D. (2019). Pemanfaatan citra penginderaan jauh untuk pemetaan daerah rawan banjir. Jurnal Geomatika, 25(1), 15–23.

Nugroho, H. A., & Sulistyowati, A. I. (2020). Integrasi SIG dan HEC-RAS untuk pemodelan banjir Sungai Serayu. Jurnal Teknik Sipil ITB.

Weng, Q. (2010). Remote Sensing and GIS Integration: Theories, Methods, and Applications. McGraw-Hill.

Hardjowigeno, S., & Widiatmaka. (2007). Evaluasi Lahan untuk Perencanaan Tata Guna Lahan. Gadjah Mada University Press.

Yulianti, M., & Fitriyah, E. (2021). Simulasi banjir menggunakan HEC-RAS berbasis DEM dan citra satelit di DAS Bengawan Solo. Jurnal Ilmu Lingkungan, 19(2), 215–